J. Astron. Space Sci. 26(1), 31-46 (2009)

Unscented KALMAN Filtering for Spacecraft Attitude and Rate Determination Using Magnetometer

Sung-Woo Kim, Mohammad Abdelrahman, Sang-Young Park†, and Kyu-Hong Choi
Astrodynamics and Control Laboratory, Yonsei University, Seoul 120-749, Korea
email: spark@galaxy.yonsei.ac.kr

(Received February 4, 2009; Accepted February 17, 2009)

Abstract

An Unscented Kalman Filter (UKF) for estimation of the attitude and rate of a spacecraft using only magnetometer vector measurement is developed. The attitude dynamics used in the estimation is the nonlinear Euler's rotational equation which is augmented with the quaternion kinematics to construct a process model. The filter is designed for small satellite in low Earth orbit, so the disturbance torques include gravity-gradient torque, magnetic disturbance torque, and aerodynamic drag torque. The magnetometer measurements are simulated based on time-varying position of the spacecraft. The filter has been tested not only in the standby mode but also in the detumbling mode. Two types of actuators have been modeled and applied in the simulation. The PD controller is used for the two types of actuators (reaction wheels and thrusters) to detumble the spacecraft. The estimation error converged to within 5 deg for attitude and 0.1 deg/s for rate respectively when the two types of actuators were used. A joint state parameter estimation has been tested and the effect of the process noise covariance on the parameter estimation has been indicated. Also, Monte-Carlo simulations have been performed to test the capability of the filter to converge with the initial conditions sampled from a uniform distribution. Finally, the UKF performance has been compared to that of the EKF and it demonstrates that UKF slightly outperforms EKF. The developed algorithm can be applied to any type of small satellites that are actuated by magnetic torquers, reaction wheels or thrusters with a capability of magnetometer vector measurements for attitude and rate estimation.

Keywords: attitude estimation, angular velocity estimation, magnetometer, unscented Kalman filter, extended Kalman filter, attitude simulator

1. Introduction

As spacecrafts nowadays become smaller and lighter, and as it is desired to make low-cost satellites, many attitude and rate determination algorithms do not lend themselves to acquiring attitude and rate measurements directly from rate gyro. Despite the rate gyro can provide very accurate angular velocity information, the gyroless attitude and rate estimation methods are strongly recommended for the reason that the rate gyro has a high possibility of malfunction (Oshman & Dellus 2003), cannot work in the case that the angular velocity of spacecrafts exceeds the saturation limit

†corresponding author

of the rate gyro, and it is too expensive for the low-cost small satellites. For example, the Earth Radiation Budget Satellite (ERBS) experienced a saturation of onboard rate gyro as a result of control anomaly during a yaw inversion maneuver, and Relay Mirror Experiment (RME) satellite suffered the similar problem after the failure of the Earth sensors (Natanson et al. 1994).

The gyroless approach for the attitude and rate estimation is being used in several missions such as solar, anomalous, and magnetospheric particle explorer (SAMPEX) satellite and the Rossi x-ray timing explorer (RXTE) satellite (Harman & Bar-Itzhack 1999). There have been several attitude and rate estimation methods that use single directional vector measurements or quaternion measurements without the rate gyro. As a part of this trend, Gai et al. (1985) suggested EKF (Extended Kalman Filter) algorithm for attitude and rate estimation only using the star sensor. This algorithm is tested based on the open-loop system and the performance has been shown to be adequate for the active stabilization of a spacecraft attitude. Another EKF algorithm using only magnetometer data was presented by Psiaki et al. (1990). In this case, the estimated states include un-modeled constant disturbance torques in addition to the attitude and rate. Their algorithm was tested using a simulation of a gravity-gradient stabilized spacecraft, and the observability and stability of the system were confirmed by a linear analysis of the system.

Several modifications to the ordinary Kalman filter have been introduced (Algrain & Saniie 1994, Julier et al. 1995, Mracek et al. 1996, Azor et al. 1998) and applied to the estimation algorithm for the attitude and rate. Some of them use one vector measurements (Psiaki et al. 1990, Psiaki 2004, Abdelrahman & Park 2008) and others use two vector measurements or a quaternion measurement (Azor et al. 1998, 2001, Harman & Bar-Itzhack 1999, Abdelrahman & Samaan 2005). Also, it has been tried to combine a deterministic algorithm with the EKF making the deterministic algorithm provide a coarse initial estimate to the EKF to address the divergence problem of the EKF when the initial estimate is poor (Oshman & Dellus 2003, Psiaki & Oshman 2003).

In this paper, an UKF (Unscented Kalman Filter) algorithm for spacecraft attitude and rate estimation has been developed using only magnetometer vector measurements. As a continuation of the research already conducted by Abdelrahman & Park (2008), this paper presents an investigation of the characteristic of estimation according to the performance of the actuators used in the simulation. The UKF is sometimes shown to be more accurate and far easier to implement than the EKF (Julier at al. 1995). Also, it does not need to calculate the SDC (State Dependent Coefficient) which is needed to implement SDREF (State Dependent Riccati Equation Filter) and PSELIKA (PSEudoLInear KAlman) filter, or to design pseudolinear model needed in the IKF (Interlaced Kalman Filter) and EIKF (Extended IKF). The performance of the UKF presented in this paper was compared to that of the EKF. The performance of the filters has been tested using a simulation of the attitude and orbit of a spacecraft in the presence of three kinds of modeled disturbances torques; gravity-gradient torque, magnetic residual torque, and aerodynamic drag torque. The attitude of the spacecraft is controlled by two types of actuators (reaction wheels and thrusters) while the estimation is performed using a magnetometer. In addition, Monte-Carlo simulations have been performed to test the performance of the filter with initial attitudes and angular velocities sampled from a uniform distribution. The presented filter has been tested not only in the standby mode when the spacecraft is stabilized but also in the detumbling mode when the spacecraft is being detumbled. The spacecraft is detumbled by a linear PD controller driven by the state estimates. To make the simulation realistic, the control torque resulted by the PD controller is generated using the two types of actuators. The control torque levels change according to the type of the actuator. The effect of the control torque level on the filter performance has been investigated using simulations.

This paper is composed by four sections. In section 2, the estimation algorithm using only magnetometer measurements is presented. Filter structure, filter tuning, and some remarks on the

parameter estimation are presented in this section. In section 3, the simulation results based on two types of actuators are explained and followed by a comparison of the performance of EKF and UKF. Also, a Monte-Carlo simulation results are shown in this section. Finally, in section 4, conclusion remarks are included.

2. Algorithms for Spacecraft Attitude and Rate Estimation

2.1 Filter Structures

The presented estimation algorithm mainly consists of the three parts; process model, measurement model, and filters (UKF and EKF). The process model includes the spacecraft dynamics model and the quaternion differential kinematics. The measurement model consists of the equations for time updating of the geomagnetic field measurement and its time derivative and it satisfies the observability with respect to the states (attitude and angular velocity). The filtering part incorporates the a priori estimate (from the process model), a measurement prediction (from the measurement model), and the magnetometer measurement to estimate the state. The algorithms of UKF and EKF are refered to Abdelrahman & Park (2008) and Zarchan & Musoff (2005) respectively.

2.1.1 Filter Process Model

The states to be estimated should have a priori estimates before they go through the filtering. The more precise the process model is, the higher prediction accuracy can be obtained. The uncertainty in the process model generally comes from the uncertainty in the dynamics model because the parameters included in the dynamics model are uncertain while on the other hand it is effected by the disturbances whose characteristics cannot be determined exactly. The process model can be constructed by combining the Euler's rotational equation and the quaternion differential kinematics as (Abdelrahman & Park 2008)

$$\begin{bmatrix} \dot{\mathbf{w}} \\ \dot{\mathbf{q}} \end{bmatrix} = \begin{bmatrix} -\mathbf{I}^{-1}\left[\mathbf{w} \times (\mathbf{I}\mathbf{w} + \mathbf{h})\right] + \mathbf{I}^{-1}\left(\mathbf{T} - \dot{\mathbf{h}}\right) \\ \frac{1}{2}\Xi(\mathbf{q})\,\mathbf{w} \end{bmatrix} + \begin{bmatrix} \mathbf{n}_w \\ \mathbf{0}_{4\times 1} \end{bmatrix} \tag{1}$$

where $\mathbf{w}$ is the spacecraft angular rate with respect to inertial frame, $\mathbf{I}$ is the spacecraft inertia tensor matrix, $\mathbf{h}$ is momentum vector of reaction wheel, $\mathbf{T}$ represents disturbance torques and control torques, $\mathbf{q}$ $(q_1 \quad q_2 \quad q_3 \quad q_4)$ is the attitude quaternion, and $\mathbf{n}_w$ is the added process noise which is assumed to be white Gaussian noise. The most important factor which contributes to the process noise is the control torque which is driven by the state estimates. So, if the control torque level increases or has an instability such as discontinuity the uncertainty in the dynamics model also increases resulting in degradation in the estimation performance. $\Xi(\mathbf{q})$ in Eq. (1) is defined as

$$\Xi(\mathbf{q}) = \begin{bmatrix} q_4\mathbf{I}_{3\times 3} + [\mathbf{q}_{13}\times] \\ \cdots \\ -\mathbf{q}_{13}^T \end{bmatrix} \tag{2}$$

where $\mathbf{q}_{13}$ represents $\begin{bmatrix} q_1 & q_2 & q_3 \end{bmatrix}^T$ and $[\mathbf{q}_{13}\times]$ is the cross product matrix.

2.1.2 Filter Measurement Model

The Measurement model is used to propagate the measurement from one time step to another. The propagated measurement can be called a predicted measurement. The difference between the predicted measurement and the true measurement obtained from the simulation of magnetometer

Table 1. Filter Tuning for UKF using Magnetometer with Reaction Wheels.

Tuning Parameter	Value
$\mathbf{P}_0$	diag [30.46 30.46 30.46 1.734 2.065 1.734 994.4] $\times 10^{-3}$
$\mathbf{Q}$	diag [1.563 1.434 1.984 0 0 0 0] $\times 10^{-14}$
$\mathbf{R}$	diag [2.500 2.500 2.500 0.1563 0.1563 0.1563] $\times 10^{-15}$
α	1
β	0
λ	0

measurement is the measurement residual which is also called an innovation. The measurement model can be represented as (Abdelrahman & Park 2008)

$$\begin{bmatrix} \mathbf{B}_b \\ \dot{\mathbf{B}}_b \end{bmatrix} = \begin{bmatrix} \mathbf{C}\mathbf{B}_i \\ \mathbf{C}\dot{\mathbf{B}}_i - \mathbf{w} \times [\mathbf{C}\mathbf{B}_i] \end{bmatrix} + \begin{bmatrix} \mathbf{n}_B \\ \mathbf{n}_{\dot{B}} \end{bmatrix} \tag{3}$$

where $\mathbf{B}_b$ is geomagnetic field vector with respect to the spacecraft frame, $\dot{\mathbf{B}}_b$ is its time derivative, $\mathbf{B}_i$ is geomagnetic field vector with respect to the inertial reference frame, $\dot{\mathbf{B}}_i$ is its time derivative, and $\mathbf{C}$ is the rotation matrix from inertial to spacecraft frame which is formulated as

$$\mathbf{C} = \left(q_4^2 - \mathbf{q}_{13}^T \mathbf{q}_{13}\right) \mathbf{I}_{3\times 3} + 2\mathbf{q}_{13}\mathbf{q}_{13}^T - 2q_4 \left[\mathbf{q}_{13}\times\right] \tag{4}$$

$\mathbf{n}_B$ and $\mathbf{n}_{\dot{B}}$ in Eq. (3) are the noise vectors related to the magnetic field measurement and its time derivative respectively. $\mathbf{n}_B$ is assumed to be white Gaussian noise with a standard deviation $\sigma_B = 50nT$ and $\mathbf{n}_{\dot{B}}$ is calculated as

$$\mathbf{n}_{\dot{B}_k} = \frac{\mathbf{n}_{B_{k+1}} - \mathbf{n}_{B_k}}{\Delta t} \tag{5}$$

where Δt is sampling time interval. Therefore, $\mathbf{n}_{\dot{B}}$ is also a white Gaussian noise. It should be noticed that in Eq. (3), the attitude information is included in the rotation matrix $\mathbf{C}$, so it is obvious that the measurement model has an observability.

2.2 Filter Tuning

To get a good performance of the filter, it has to be tuned appropriately. The tuning factors of the filter include initial state error covariance $\mathbf{P}_0$, process noise covariance $\mathbf{Q}$, and measurement noise covariance $\mathbf{R}$. For the UKF, α, β, λ are included additionally in the tuning parameters. These are the scaling factors used to calculate the weights used in the UKF algorithm. α determines the spread of the sigma points, β is used to incorporate the prior knowledge about the distribution of the states (Abdelrahman & Park 2008) and λ is used to scale the fourth order moment (and higher order even moments) of the sigma points distribution (Julier et al. 1995).

Each tuning factor has its role in the filtering process. $\mathbf{P}_0$ determines how fast the estimator converges initially and has no responsibility for the filter performance in the steady state. $\mathbf{Q}$ and $\mathbf{R}$ determines the tradeoff between the rapid tracking the state variations under the disturbance noise and the filtering of the measurement noise. In addition, $\mathbf{Q}$ and $\mathbf{R}$ also determines the filter stability in the steady state (Psiaki et al. 1990). The convergence speed is one of many factors that are used in evaluation of the filter performance in real-time. To make a filter converge rapidly, $\mathbf{P}_0$ or $\mathbf{Q}$ have to be set large compared to $\mathbf{R}$. However, $\mathbf{Q}$ and $\mathbf{R}$ affects the steady state performance of the filter. So, $\mathbf{P}_0$ has been set large compared to $\mathbf{R}$ in a time-varying filter, like the EKF, to make the filter converge fast without any loose of filtering optimality in the steady state (Psiaki et al. 1990).

Table 2. Filter Tuning for UKF using Magnetometer with Thrusters.

Tuning Parameter	Value
$\mathbf{P}_0$	diag[25.78 25.78 25.78 1.467 1.748 1.467 841.7] $\times 10^{-3}$
$\mathbf{Q}$	diag[7.805 7.164 9.909 0 0 0 0] $\times 10^{-14}$
$\mathbf{R}$	diag[2.500 2.500 2.500 0.1563 0.1563 0.1563] $\times 10^{-15}$
α	1
β	0
λ	0

Table 3. Filter Tuning for EKF using Magnetometer with Thrusters.

Tuning Parameter	Value
$\mathbf{P}_0$	diag [154.4 154.4 154.4 8.790 10.47 8.790 5041
$\mathbf{Q}$	diag [7.910 7.261 10.04 0 0 0 0] $\times 10^{-14}$
$\mathbf{R}$	diag [2.500 2.500 2.500 0.1563 0.1563 0.1563] $\times 10^{-15}$

In Table 1 and 2, the tuning parameters are presented for UKF according to actuators used in the simulation. The process noise and initial error covariance for each actuator have been chosen to reflect the different system characteristics resulted from the different control torque. The tuning parameters for EKF are presented in Table 3 and it is noticed that the initial error covariance for EKF is set much larger than for UKF. The EKF is very sensitive to the initial state error, so the initial state error covariance $\mathbf{P}_0$ should be carefully tuned for EKF. In addition, the calculated error covariance matrix in the EKF does not necessarily represent the true error covariance (Banani & Masnadi-Shirazi 2007). On the other hand the UKF is not affected significantly by the initial error covariance. In this paper, while comparing the performance of the UKF and the EKF, each filter has been tuned separately to produce the best results for each filter.

2.3 Some Remarks on Parameter Estimation

The parameters used in modeling of a system generally are not known exactly. So the process and measurement models used in estimation algorithms have some uncertainties in themselves. Some parameters are represented explicitly in the model equations. In this case the parameter can be directly estimated. On the other hand, for the parameters which are not expressed in an explicit form, the uncertainties of them can be represented, in estimation theory, by the process noise covariance and the measurement noise covariance. Then, these noise covariances can be considered as parameters which should be tuned or estimated to produce a near optimal performance of the filter. No matter what kind of parameter it is, the one which appears explicitly in the model or the noise covariance, there have been two ways to estimate these parameters. In one way, the parameters are included in the state vector and estimated with the states. This joint state parameter estimation problem has been presented by Psiaki et al. (1990). The other way is to separate the estimation algorithm into two parts; one part for state estimation and the other part for parameter estimation. In this approach, the filter estimate the states with the parameters which is estimated from the other filter designed and run for parameter estimation, and the estimated states is fed back in turn to the other filter for parameter estimation. This method is called dual estimation and has been used by Song et al. (2007).

In this paper, the estimation of the drag coefficient (C_d) and the spacecraft dipole moment ($\mathbf{m}$)

Table 4. Simulation Parameters.

Simulation Parameter	Value
Initial Attitude	$[\ 10 \quad 120 \quad 30\ ]^T$ deg
Initial Angular Velocity	$[\ -4 \quad -4 \quad -2\ ]^T$ deg/s
Initial Rate Estimate	$[\ 0 \quad 0 \quad 0\ ]^T$ deg/s
Initial Attitude Estimate	$[\ 0 \quad 0 \quad 0\ ]^T$ deg
Initial Position	$[\ -1220 \quad -966.5 \quad 6854\ ]^T$ km
Initial Velocity	$[\ -7.426 \quad 0.1801 \quad -1.277\ ]^T$ km/s
Inertia Tensor	diag $[\ 9.80665 \quad 9.80665 \quad 9.80665\ ]^T$ kgm^2
Spacecraft Dipole Moment	$[\ 0.3 \quad 0.3 \quad 0.3\ ]^T$ Am^2
Drag Coefficient	2
Simulation Start Time	2007.04.17 22h 30m
Sampling Time	4 sec
Simulation Time Span	18000 sec

have been incorporated. They can be included in the state vector as

$$\mathbf{x} = [\ \mathbf{w} \quad \mathbf{q} \quad C_d \quad \mathbf{m}\ ]^T \tag{6}$$

to make the problem a joint state parameter estimation problem. Then the filter process model which propagates the augmented state vector in Eq. (6) becomes

$$\begin{bmatrix} \dot{\mathbf{w}} \\ \dot{\mathbf{q}} \\ \dot{C}_d \\ \dot{\mathbf{m}} \end{bmatrix} = \begin{bmatrix} -\mathbf{I}^{-1}\left[\mathbf{w} \times (\mathbf{I}\mathbf{w} + \mathbf{h})\right] + \mathbf{I}^{-1}\left(\mathbf{T} - \dot{\mathbf{h}}\right) \\ \frac{1}{2}\boldsymbol{\Xi}(\mathbf{q})\ \mathbf{w} \\ 0 \\ 0 \end{bmatrix} + \begin{bmatrix} \mathbf{n}_w \\ \mathbf{0}_{4\times 1} \\ \mathbf{n}_{C_d} \\ \mathbf{n}_m \end{bmatrix} \tag{7}$$

where C_d and $\mathbf{m}$ are considered to have no dynamics; even if there is some dynamics regarding these parameters, there is no way to know it. All the noise in Eq. (7) has been considered as a white Gaussian noise.

The discrete process noise covariance has been applied instead of the continuous one (diagonal matrix) to see the effect of the off diagonal elements on the parameter estimation. The discrete process noise covariance matrix does not become a diagonal matrix with some elements in off-diagonal parts and this makes the estimates for parameters change its value while they do not change in application of continuous process noise covariance. However, to get the satisfactory performance of estimation for these parameters, the off-diagonal elements in the process noise covariance matrix have to be tuned appropriately. This problem has not been solved yet, so in this paper just the variation of the estimates for parameters will be shown to demonstrate the effect of the off diagonal elements on the parameter estimation. The simulation results are presented in section 3.

3. Simulations and Results

3.1 Simulation Environments and Parameters

The simulation environments and parameters in Table 4 are based on the EgyptSat-1 mission. The simulation assumes a small satellite whose only measurement device is the magnetometer. Its attitude is controlled by a PD controller using two types of actuators. The orbit is assumed to be a sun synchronous polar orbit of 688 km altitude, 98.085 deg inclination, and 0.001 eccentricity.

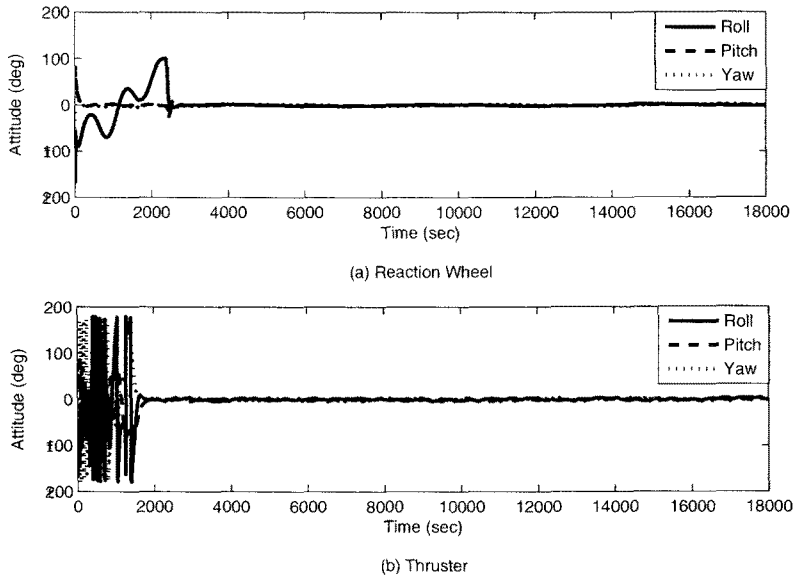

Figure 1. Attitude Simulation with (a) Reaction Wheels and (b) Thrusters.

Simulation test period is divided into detumbling mode and standby mode. After the spacecraft is separated from the launcher the detumbling mode begins and last until the attitude and angular velocity of the spacecraft is decreased to within certain boundaries. The pitch momentum wheel starts to spin up at the time of the separation and maintain the constant pitch momentum of 0.1 Nms. The simulation has been done during 18,000 sec which is corresponding to about three orbits. The inertia tensor of the spacecraft is assumed to be a diagonal matrix and the sampling time is set to be 4 sec which is relatively large. The true states (attitude and angular velocity) are obtained through a simulation of an on-board rate gyro, then the difference between true states and the states estimated using a three-axis magnetometer is calculated to produce the estimation error.

3.2 Attitude Controls with Two Types of Actuators

The attitude of the spacecraft is controlled by a PD controller which is represented as (Abdelrahman & Park 2008)

$$\mathbf{T}_c = -\mathbf{K}_p q_{4e}^{br} \mathbf{q}_{13e}^{br} - \mathbf{K}_v \mathbf{w}^{br} \tag{8}$$

where $\mathbf{K}_p$ and $\mathbf{K}_v$ are control gains and, $\mathbf{q}_{13e}^{br}$ is a vector composed of the first three components of the error attitude quaternion $\mathbf{q}_e^{br}(\ q_{1e}^{br} \quad q_{2e}^{br} \quad q_{3e}^{br} \quad q_{4e}^{br}\ )$ of the spacecraft with respect to orbital reference frame and $\mathbf{w}^{br}$ is spacecraft angular rate vector with respect to orbital reference frame. The error attitude quaternion is formulated using quaternion multiplication rule as

$$\mathbf{q}_e^{br} = \mathbf{q}^{br} \otimes \mathbf{q}_T^{-1} = \begin{bmatrix} q_{4T}\mathbf{q}_{13}^{br} - q_4^{br}\mathbf{q}_{13T} + \mathbf{q}_{13}^{br} \times \mathbf{q}_{13T} \\ \cdots\cdots\cdots\cdots\cdots \\ q_4^{br} q_{4T} + \mathbf{q}_{13}^{br} \cdot \mathbf{q}_{13T} \end{bmatrix} \tag{9}$$

where $\mathbf{q}_T^{-1}$ is an inverse of the target attitude quaternion resolved in the orbital reference frame. The

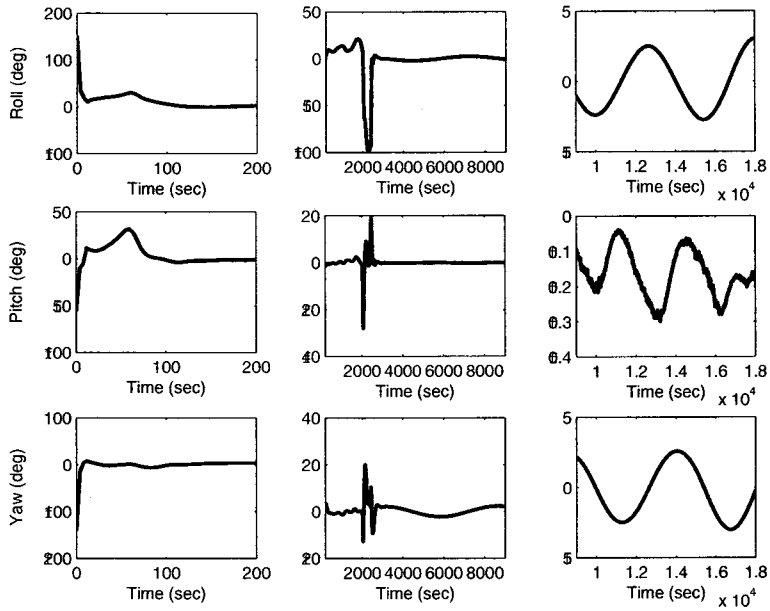

Figure 2. UKF Attitude Estimation Error using Magnetometers with Reaction Wheels.

attitude quaternion $\mathbf{q}^{br}$ and the angular velocity $\mathbf{w}^{br}$ used in Eq. (9) and Eq. (8) are the estimated states.

The control torque calculated by the PD controller provides an input to each type of actuator. In this section, attitude control simulation results using the two types of actuators are presented. In this simulation the spacecraft is assumed to have initial momentum of 0.1 Nms along the pitch axis. The initial attitude and angular velocity are [10 120 30] deg and [−4 −4 −2] deg/s respectively, and control target is [0 0 0] deg. The histories of true attitude controlled by reaction wheels and thrusters are shown in Figure 1. The reaction wheels and thrusters reduced attitude pointing error to 3 deg and 4 deg respectively. The accuracies of attitude controls is worse than general case because a PD controller is applied to the nonlinear systems.

3.3 Attitude Estimations using Magnetometer

The estimation results of the UKF using magnetometer are presented in this section. It has been shown that the performance of the UKF can be affected by the control torque level significantly. The steady state estimation errors are converged when the two types of actuators are used. The simulation results using the two types of actuator will be explained in the next subsections.

3.3.1 Attitude Estimation Results from Reaction Wheels Utilization

The UKF estimation results using magnetometers are presented in Figure 2 and 3 when the reaction wheels are used as actuators, and the relevant filter tuning is presented in Table 1. Each reaction wheel along the three axes is assumed to be able to generate a maximum control torque of 0.02 Nm and a maximum wheel momentum of 1 Nms. Figure 4a shows the control torque level when the reaction wheel is used. The effects of the control torque level on the estimation accuracy can be recognized by comparing Figure 4a and Figure 2 and 3. As it is shown in Figure 4a, the

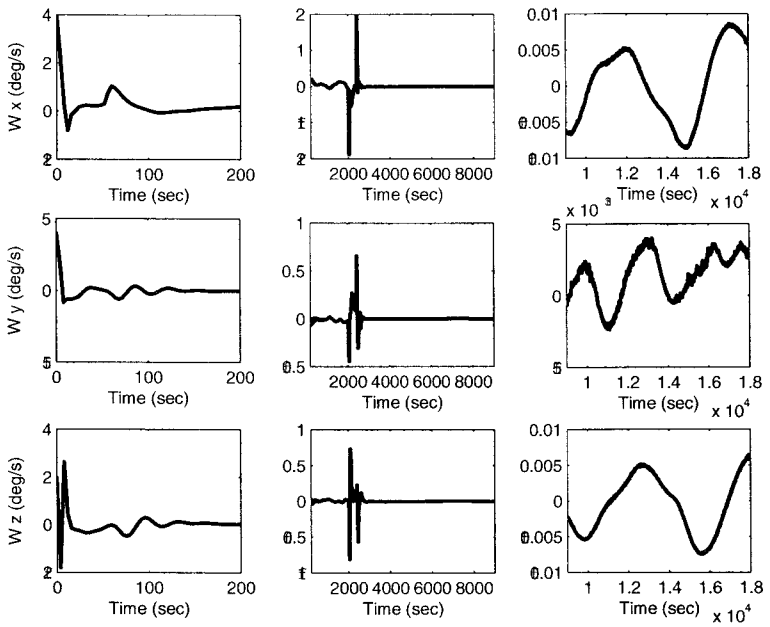

Figure 3. UKF Angular Velocity Estimation Error using Magnetometers with Reaction Wheels.

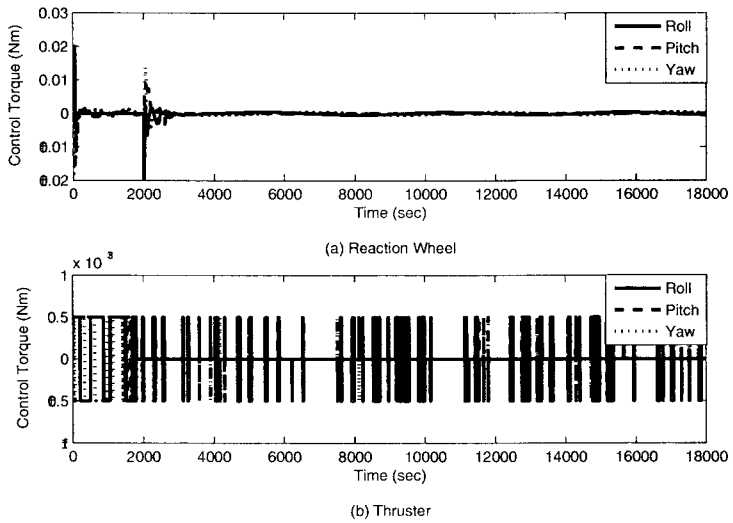

Figure 4. Control Torque Level driven by UKF Estimate using Magnetometers with (a) Reaction Wheels and (b) Thrusters.

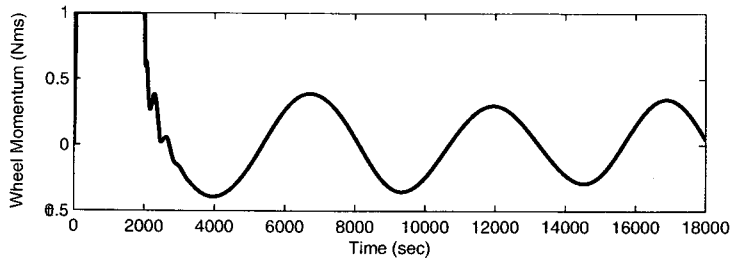

Figure 5. Roll Axis Momentum of Wheel.

control torque level suddenly increases and makes a pick up to 0.02 Nm in its magnitude. This jump in the control torque level is because of the saturation of roll momentum of reaction wheel. The saturation occurs at about 2000 sec as shown in Figure 5. This rapid change in control torque makes the estimation error increase high up to 100 deg and 2 deg/s for attitude and rate respectively as shown in Figure 2 and 3. After 2,000 sec, the estimation error again decreases to the level as it was before 2,000 sec and maintains the level (3 deg, 0.01 deg/s for each axis) for the rest. It is noticed that the steady state estimation accuracy of the attitude angle about the pitch axis is better than the attitude angles about the other axes. The reason of this is thought to be the fact that the spacecraft is pitch biased.

3.3.2 Attitude Estimation Results from Thrusters Utilization

The UKF estimation results using magnetometers are presented in Figure 6 and 7 when the thrusters are used as actuators, and the relevant filter tuning is presented in Table 2. The thrusters are assumed to be able to generate the constant magnitude of control torque (0.0005 Nm) about all three axes every 4 sec. There are no jumps in the control torques appearing in the case of reaction wheel application, so any failure of estimation due to the sudden increase in the estimation error is not shown. The estimation error for attitude and angular velocity converged to within 5 deg and 0.1 deg/s respectively for each axis at about 2,000 sec and maintain that accuracy to the end of simulation. However, the control torque level is highly nonlinear as it is shown in Figure 4b because the thrusters control the attitude only changing the direction of the control torque and is designed not to work when the attitude pointing error is less than 4 deg in magnitude. This nonlinearity in the control torque affects the performance of the filter raising the steady state estimation errors slightly higher than the errors obtained when the reaction wheel is applied as actuator, even though the control torque levels in steady state are about 5×10^{-4} Nm for both actuators.

3.3.3 Comparison Between UKF and EKF

A comparison of the estimation performance of the magnetometer between UKF and EKF has been done when the thrusters are used as actuators. Each filter has been tuned separately to produce its best performance. In Figure 8 and 9, the UKF and EKF estimation error RMS (Root Mean Squares) has been compared. The first panels in Figure 8 and 9 cover from the start to 200 sec, the second panels cover from 200 to 2,000 sec, and the third panels cover from 2,000 sec to the end. It is shown in Figure 9 that the initial convergence is more rapid in UKF than in EKF. After 200 sec, the history of estimation error RMS of the UKF is almost the same with that of EKF. Both filters could reduce the steady state error RMS to within 5 deg and 0.1 deg/s for attitude and angular velocity respectively.

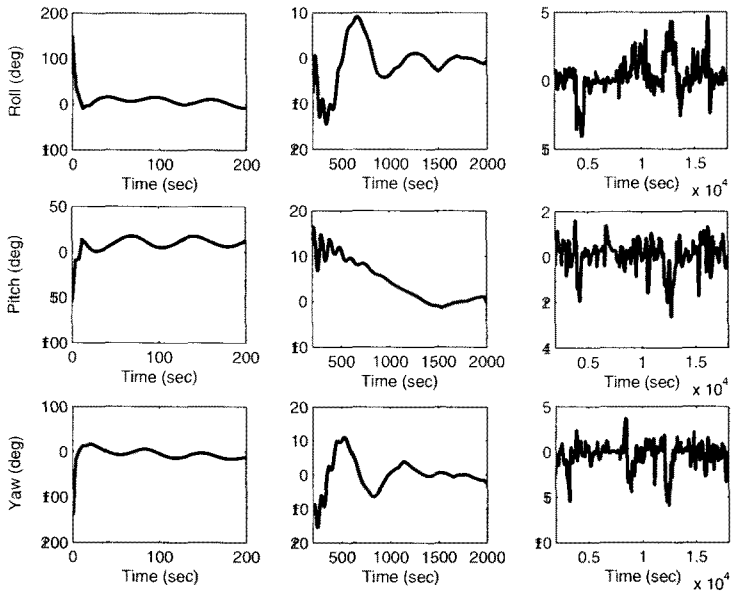

Figure 6. UKF Attitude Estimation Error using Magnetometers with Thrusters.

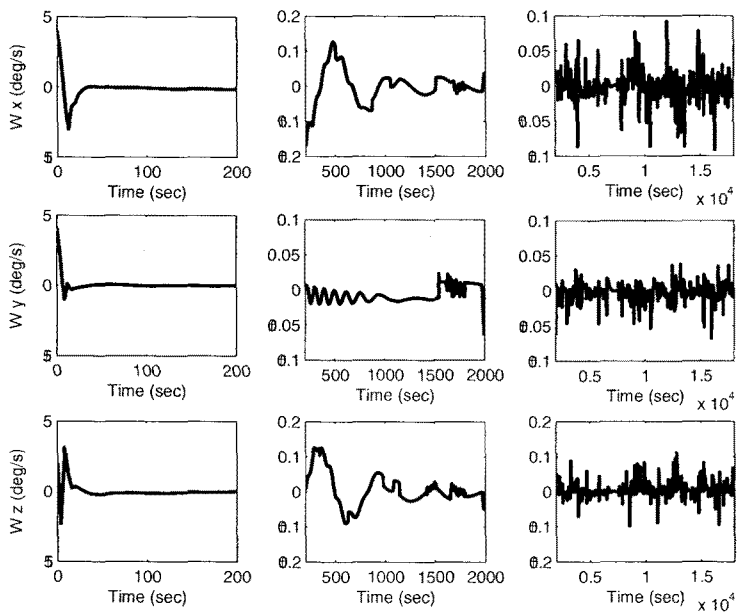

Figure 7. UKF Angular Velocity Estimation Error using Magnetometers with Thrusters.

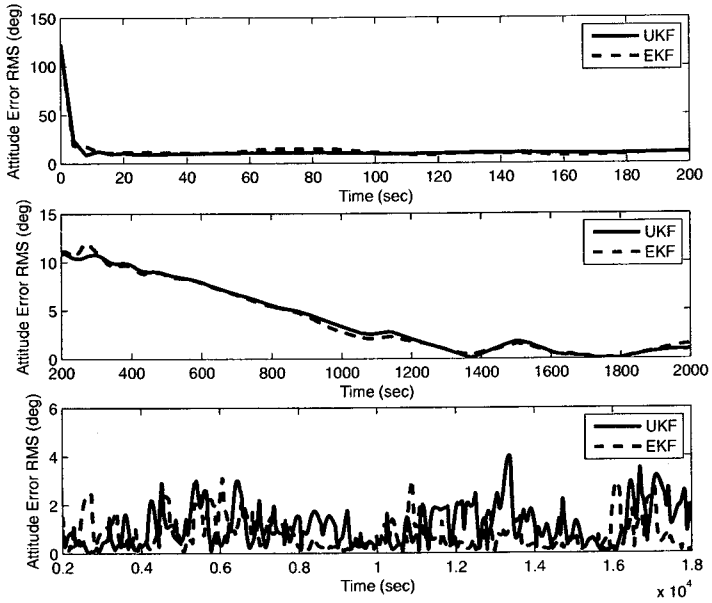

Figure 8. RMS of Attitude Estimation Error for the UKF and EKF using Magnetometers with Thrusters.

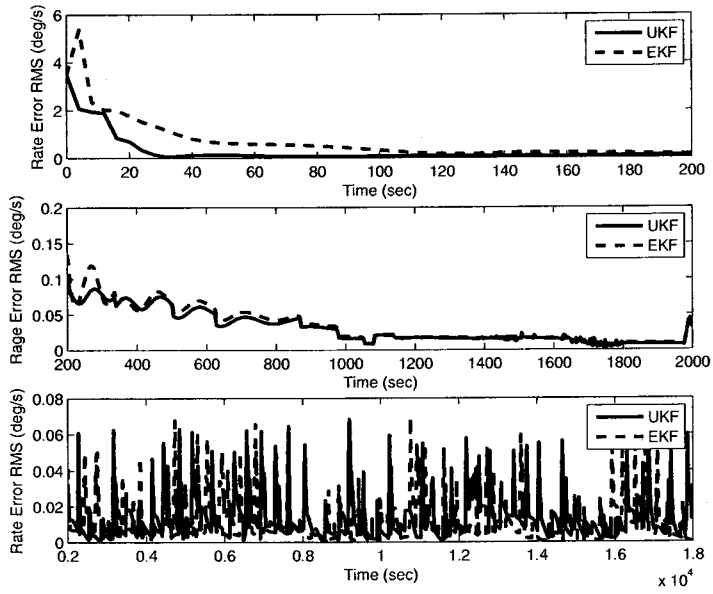

Figure 9. RMS of Angular Velocity Estimation Error for the UKF and EKF using Magnetometers with Thrusters.

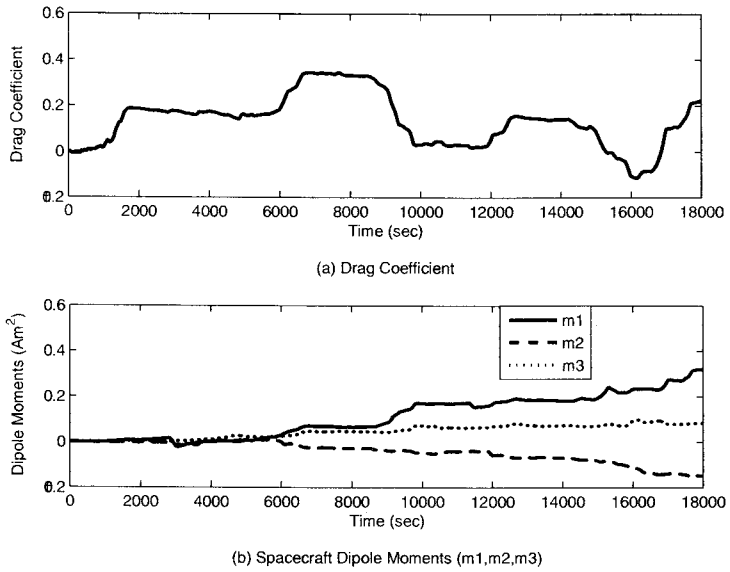

Figure 10. Variation of the Estimates for Parameters; (a) Drag Coefficient and (b) Spacecraft Dipole Moments.

3.4 Variation of the Parameter Estimates

The effects of the process noise covariance on the estimation of C_d and $\mathbf{m}$ has been demonstrated by a simulation. Thrusters are used as actuators in this simulation. The continuous and discrete process noise covariance matrices have been applied in the UKF algorithm and compared to show the effects of the off diagonal elements in the process noise covariance matrix on the parameter estimation. The parameter estimate does not change its value from initial estimate ($\hat{C}_{d0} = 0, \hat{\mathbf{m}}_0 = [\ 0 \quad 0 \quad 0\ ] Am^2$) when the diagonal constant process noise covariance matrix is used, while the discrete process noise covariance matrix (it has off diagonal elements) forces the parameter estimate to change its value. The off diagonal elements of the discrete process noise covariance matrix represent the correlation between the states and parameters. If this correlation is neglected (i.e.,zero off diagonal elements), the measurement model loses its observability with respect to the parameters (C_d and $\mathbf{m}$) resulting in the failure of the estimation. This fact has been verified by a simulation. The simulation results are presented in Figure 10 where the variations of the parameter estimates are shown when the discrete process noise covariance matrix is used. However the estimation could not track the true value of the parameters. For the better performance in the parameter estimation, the process noise covariance matrix should be tuned well.

3.5 Monte-Carlo Simulation Results

A Monte-Carlo simulation has been done to verify the capacity of the UKF to converge with various initial conditions. The maximum value of the RMS of attitude and angular velocity errors are chosen from one orbit period of standby mode. In this simulations the thrusters are used as actuators. The initial attitude has been sampled from the uniform distribution ranging from –120 deg to 120 deg, and the initial angular velocity also has been sampled from the uniform distribution ranging from –5 deg/s to 5 deg/s. In Figure 11 and 12, the simulation results for the attitude and the angular velocity are presented respectively. The maximum attitude error RMS for three axes is

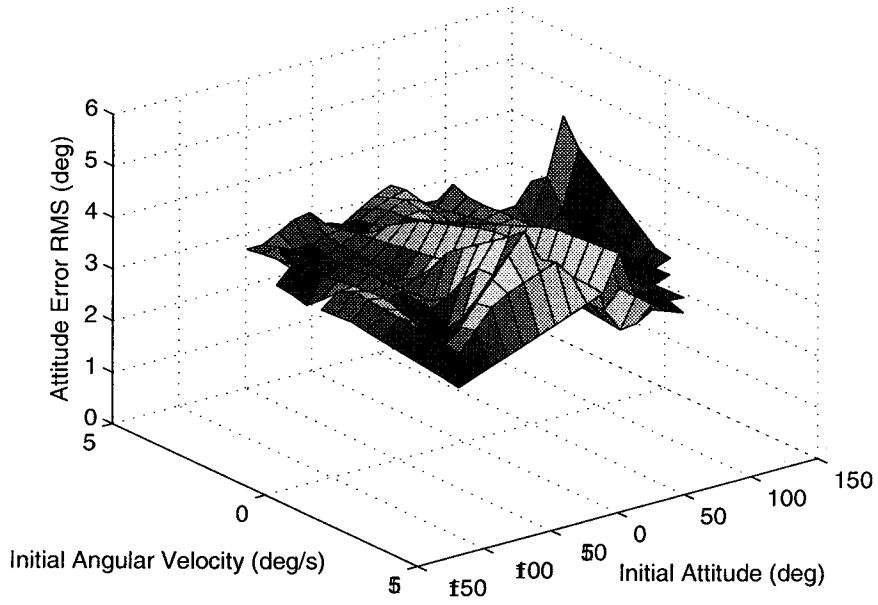

Figure 11. Monte-Carlo Simulation for Attitude Estimation using the UKF.

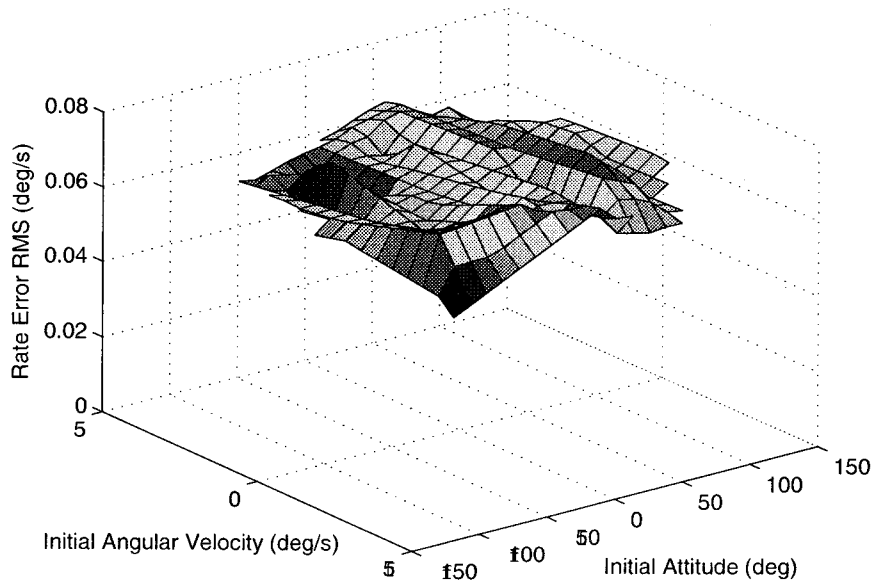

Figure 12. Monte-Carlo Simulation for Angular Velocity Estimation using the UKF.

shown to be 5.5023 deg, and the maximum angular velocity error RMS for three axes is shown to be 0.0779 deg/s. So, it has been demonstrated that the UKF is stable for the various initial state error.

4. Conclusions

An UKF algorithm for estimation of the spacecraft attitude and rate only using magnetometer measurement has been developed and tested. It has been noticed that the filter performance is strongly affected by the control torque level through the simulation using two types of actuators (reaction wheels and thrusters). The steady state estimation error of 3 deg, 0.01 deg/s (reaction wheels) and 5 deg, 0.1 deg/s (thrusters) have been obtained for attitude and rate respectively for each axis while the spacecraft is detumbled by a PD controller. The performance of the UKF algorithm has been compared to that of the EKF. The UKF demonstrates its advantages to the EKF in rapid initial convergence of the angular velocity estimate. The estimate error of UKF converges about 100 sec faster than that of EKF. Also, a Monte-Carlo simulation has been done to verify the stability of the UKF for various initial state errors. As a result, the attitude error RMS for three axes did not exceed 5.5023 deg and the angular velocity error RMS for three axes did not exceed 0.0779 deg/s for the specified environments.

The parameter estimation problem has been mentioned briefly as a joint state parameter estimation problem. The spacecraft dipole moment and drag coefficient have been included in the state to be estimated. However, it has not been completed to find adequate process noise covariance matrix for estimation of C_d and $\mathbf{m}$. Nevertheless, it was noticed that the off diagonal elements of the process noise covariance matrix play an important role in tracking the parameters. The developed algorithm throughout the paper can be used in any type of small satellite equipped with magnetic torquers, reaction wheels or thrusters as actuator and the magnetometer for attitude and rate estimation.

Acknowledgements: This work is supported by the Korean Science and Engineering Foundation (KOSEF) through the National Research Laboratory Program funded by the Ministry of Science and Technology (No. M10600000282-06j0000-28210).

References

Abdelrahman, M. & Park, S-Y. 2008, submitted to IEEE Transactions on Aerospace and Electronic Systems

Abdelrahman, M. & Samaan, M. A. 2005, in ACSE-05, ed. A. Aboshosha (Cairo: CICC), p.47

Algrain, M. C. & Saniie, J. 1994, IEEE Transactions on Aerospace and Electronic Systems, 30, 175

Azor, R., Bar-Itzhack, I. Y., Deutschmann, J. K., & Harman, R. R. 2001, JGCD, 24, 436

Azor, R., Bar-Itzhack, I. Y., & Harman, R. R. 1998, JGCD, 21, 450

Banani, S. A. & Masnadi-Shirazi, M. A. 2007, in WASET (Barcelona: WASET), p.192

Gai, E., Daly, K., Harrison, J., & Lemos, L. 1985, JGCD, 8, 560

Harman, R. R. & Bar-Itzhack, I. Y. 1999, JGCD, 22, 723

Julier, S. J., Uhlmann, J. K., & Durrant-Whyte, H. F. 1995, in IEEE ACC-1995 (Seattle: IEEE), p.1628

Mracek, C. P., Cloutier, J. R., & D'Souza, C. A. 1996, in IEEE ICCA-1996, ed. O. R. Gonzalez (Michigan: CSS), p.338

Natanson, G. A., Challa, M. S., Deutschmann, J., & Baker, D. F. 1994, in International Symposium on Space Mission Operations and Ground Data Systems, ed. J. L. Rash (Maryland: Goddard Space Flight Center), p.791

Oshman, Y. & Dellus, F. 2003, JSR, 40, 237
Psiaki, M. L. 2004, JGCD, 27, 240
Psiaki, M. L., Martel, F., & Pal, P. K. 1990, JGCD, 13, 506
Psiaki, M. L. & Oshman, Y. 2003, JGCD, 26, 244
Song, Q., Jiang, Z., & Han, J. 2007, in IEEE ICRA-2007 (Roma: IEEE), p.4164
Zarchan, P. & Musoff, H. 2005, Fundamentals of Kalman Filtering: A Practical Apporach 2nd edition (Virginia: AIAA), pp.257-259